JAAS

Fundamentals and new approaches to calibration in atomic spectrometry

Journal:	*Journal of Analytical Atomic Spectrometry*
Manuscript ID	JA-TRV-08-2019-000273.R1
Article Type:	Tutorial Review
Date Submitted by the Author:	10-Sep-2019
Complete List of Authors:	Donati, George; Wake Forest University, Chemistry Amais, Renata S; State University of Campinas Institute of Chemistry

SCHOLARONE™
Manuscripts

Fundamentals and new approaches to calibration in atomic spectrometry

George L. Donati*[,a] and Renata S. Amais[b]

[a]Department of Chemistry, Wake Forest University,

Salem Hall, Box 7486, Winston-Salem, NC 27109, USA

[b]Spectrometry, Sample Preparation and Mechanization Group (GEPAM), Institute of Chemistry,

University of Campinas, PO Box 6154, Campinas, SP 13083-970, Brazil

*Corresponding author: e-mail: donatigl@wfu.edu. Tel.: +1 336 758-4815. Fax: +1 336 758-4656.

Abstract

Despite efforts to develop calibration-free methods for atomic spectrometry, the most successful applications of quantitative instrumental techniques involve calibration. In this review paper, we discuss the principles and applications of both traditional and some recently described calibration methods as they are used in spectrochemical analysis. We particularly focus on the fundamentals, basic conditions and statistics of linear regression based on least-squares fitting, including the impact of normality and heteroscedasticity on accuracy. Advantages and limitations of the external standard calibration (EC), internal standardization (IS) and standard additions (SA) methods are critically discussed, as well as new calibration strategies such as interference standard (IFS), standard dilution analysis (SDA), multi-energy calibration (MEC), multi-isotope calibration (MICal), multispecies calibration (MSC) and multi-flow calibration (MFC).

List of contents

Introduction 1

Fundamentals of least-squares regression 2

Impact of heteroscedasticity on accuracy 5

Advantages and limitations of the traditional calibration methods used in atomic spectrometry 7

External standard calibration (EC) and matrix matching calibration (MMC) 7

Internal standardization (IS) 9

Standard additions (SA) 11

Some recently proposed strategies to improve calibration efficiency in atomic spectrometry 15

Interference standard method (IFS) 15

Standard dilution analysis (SDA) 17

Multi-signal methods 19

Main advantages and limitations of IFS, SDA and the multi-signal methods 24

Calibration methods with both variables subject to error 26

Conclusions and perspectives 27

Abbreviations

CRM	Certified reference material
EC	External standard calibration
FAAS	Flame atomic absorption spectrometry
FAES	Flame atomic emission spectrometry
FMAS	Flame molecular absorption spectrometry
GF AAS	Graphite furnace atomic absorption spectrometry
GF MAS	Graphite furnace molecular absorption spectrometry
HR-CS	High resolution continuum source
HR-SF	High resolution sector field
ICP-QMS	Inductively coupled plasma quadrupole-based mass spectrometry
ICP-MS	Inductively coupled plasma mass spectrometry
ICP-MS/MS	Inductively coupled plasma tandem mass spectrometry
ICP OES	Inductively coupled plasma optical emission spectrometry
IFS	Interference standard
IS	Internal standardization or Internal standard
LA-ICP-MS	Laser ablation inductively coupled plasma mass spectrometry
LIBS	Laser-induced breakdown spectroscopy
LOD	Limit of detection

MEC	Multi-energy calibration
MFC	Multi-flow calibration
MICal	Multi-isotope calibration
MIP OES	Microwave-induced plasma optical emission spectrometry
MMC	Matrix matching calibration
MSC	Multispecies calibration
ODR	Orthogonal distance regression
OLS	Ordinary least-squares regression
RSD	Relative standard deviation
RSMSE	Root-mean-square error
SA	Standard additions
SDA	Standard dilution analysis
WLS	Weighted least-squares regression

Introduction

Almost all atomic spectrometry techniques exploit quantized transitions, which are characteristic of each individual element and are instrumentally detectable in most cases. Modern quantitative analysis methods are based on the relationship between instrument response and analyte concentration. This relationship is heavily influenced by physical parameters specific to the analyte and to the type of analytical technique used, as well as by instrumental conditions and matrix effects.[1] Therefore, despite efforts to develop calibration-free methods,[2-4] the most successful applications of quantitative instrumental techniques involve calibration.

For most spectrochemical analysis methods, instrument response and analyte concentration present a linear relationship within a certain concentration range (linear dynamic range). Thus, calibration involves using a few standard solutions of known analyte concentration to estimate the parameters of the linear function describing this relationship.[5,6] In the present work, we discuss the fundamentals and statistics of linear regression based on least-squares fitting, as it is applied to the most traditional calibration methods used in atomic spectrometry. We also explore the main advantages and limitations of external standard calibration (EC), internal standardization (IS), and the standard additions method (SA). Finally, we discuss the fundamentals and applications of some new calibration strategies including the interference standard method (IFS), standard dilution analysis (SDA), multi-energy calibration (MEC), multi-isotope calibration (MICal), multispecies calibration (MSC), and multi-flow calibration (MFC). An overview of the calibration methods discussed here is presented in Table 1.

The present work is not meant to be a comprehensive review of all calibration methods employed in atomic spectrometry. We do not examine, for example, multivariate approaches such as partial least-squares regression, principal component analysis, principal component regression

and other chemometric-based strategies.[7,8] It is also important to note that, for the traditional EC, IS and SA, we discuss applications in a more general sense, with no focus on specific issues associated with a particular atomic spectrometry technique. For additional details, for example, on strategies for correcting signal bias and improving calibration in laser-sampling-based methods such as laser-induced breakdown spectroscopy (LIBS) and combinations of laser ablation (LA) with inductively coupled plasma optical emission spectrometry (ICP OES) and inductively coupled plasma mass spectrometry (ICP-MS), the reader is referred to some thorough and comprehensive works recently published.[9,10]

Fundamentals of least-squares regression

Calibration, as it is commonly used in a variety of atomic spectrometry applications, owes its existence to the concept of least-squares regression, which was first described by Legendre in 1805.[11] Galton, however, was perhaps the first researcher to actively apply linear regression to fit experimental data in 1877.[12] The birth of modern quantitative spectrochemical analysis is usually attributed to Hartley, who used a spark source to determine Be in Ce compounds in 1882.[13,14] Quantitative determination was relatively difficult at that time because of the instability of atomization sources available and the consequent effects on accuracy and precision. Therefore, some authors argue that modern quantitative spectrochemical analysis only became a reality after the introduction of the concept of internal standardization by Gerlach in 1925.[13-15] The first mention of using least-squares regression in Analytical Chemistry was in a paper by Youden in 1947,[16] with an example of such application in spectrophotometry, for example, as early as 1955.[17]

Traditional calibration methods such as EC and IS employ least-squares linear regression to estimate the functional parameters used to determine the concentration of analyte in the samples (more details on how these parameters are estimated according to least-squares fitting are presented in the Supplementary Material). In most laboratories, the analyte concentration in the sample is automatically calculated using the instrument software, or by determining the calibration curve's functional parameters using popular software packages such as Microsoft Excel. Due to the availability and simplicity of these software applications, analysts often perform linear regression based on least-squares fitting without deliberately thinking about its potential limitations or how it generally works.

Calibration curves based on least-squares regression (also known as ordinary least-squares regression, OLS) assume three important conditions for which it can be successfully applied:

1. *Only the instrument response (y-axis) is subject to error. Errors in analyte concentration (x-axis) are negligible*. Considering that instrument response error usually ranges between 1% and 5 %, while concentration errors are *ca.* 0.1 % or better, this assumption is valid for most applications. In addition, analyte concentration accuracy can be further improved, when necessary, by preparing solutions by mass rather than the traditional mass and volume approach.

2. *Instrument response error is normally distributed.* This assumption is valid for most atomic spectrometry determinations. Unless a systematic error is present due to instrument or matrix effect issues, analytical signal error is generally Gaussian, *i.e.* normally distributed. This is the case because the overall signal fluctuation in atomic spectrometry measurements comes from a combination of noise sources. As a consequence of the central limit theorem, each individual noise may not be normally distributed, but their combination, which results in the overall measurement error, is.[6,18]

3. *The magnitude of the errors in instrument response are independent of analyte concentration, i.e. errors in instrument response should not increase with increasing analyte concentration*. This condition, known as homoscedasticity (as opposed to heteroscedasticity), is not always satisfied in atomic spectrometry. Often, the error in instrument response, S_y, increases with analyte concentration.

If S_y is proportional to y, one can correct for heteroscedasticity by using $\sqrt{y}$ and $\sqrt{x}$ to respectively replace the original y (instrument response) and x (analyte concentration) values to build the calibration curve. On the other hand, if S_y is proportional to y^2, which often results in constant relative standard deviation (RSD) values and is the most common case in atomic spectrometry, homoscedastic conditions may be achieved by using *log y* and *log x* to build the calibration curve. These types of transformation, however, may deviate the relationship between instrument response and analyte concentration from linearity, and are not recommended in atomic spectrometry applications.[6] In such cases, the most effective approach to correct the analytical signals and promote homoscedasticity is to employ weighted least-squares regression (WLS), which is based on introducing weighting factors, w, inversely proportional to the source of heteroscedasticity. For example, $w = 1/y$ or $w = 1/y^2$ would be included in the estimation of slope and intercept if S_y is proportional to y, or to y^2, respectively.[6] Some modern instruments already include this type of correction as part of their controlling software, allowing the user to choose between unweighted (OLS) and weighted (WLS) least-squares regression with an assortment of weighting factors. An important potential issue with this approach is associated with sensitivity. When WLS regression is used, the regression line is forced to track closer to points with the lowest S_y values. If S_y is proportional to y or y^2, the lower-concentration standards will be more important (higher weight) in the regression. Therefore, one must be careful while choosing the concentrations

of the standard solutions used to build the weighted calibration curve, and ensure that the lower-concentration points are significantly higher than the analytes' limits of detection (LODs) to prevent biased results.

Impact of heteroscedasticity on accuracy

The three conditions discussed earlier for appropriate use of OLS regression are especially relevant when determining regression statistics. Confidence intervals for slope, intercept and the expected concentration of analyte in the sample, for example, are all calculated from Student's *t* and *F* statistics, which are both based on normal distribution and homoscedasticity. On the other hand, mean analyte concentrations calculated from either OLS or WLS regressions are usually very similar.[6] In the end, heteroscedasticity does not cause bias to the average OLS coefficients, even though their values are no longer the ones with minimum variance possible. In other words, the mean coefficient values estimated from heteroscedastic data should not affect accuracy, although their standard deviations, S_b and S_m (for the intercept, b, and the slope, m), will be biased, leading to biased test statistics and biased confidence intervals.[19]

Despite the potential issues with heteroscedasticity, according to an extensive study by Bohrnstedt and Carter, OLS regression results will be unaffected unless severe deviation from homoscedasticity is present.[20] Thus, the fact that OLS (not WLS) is broadly used in atomic spectrometry calibration is associated to (*i*) OLS regression involves much simpler calculations than WLS; (*ii*) heteroscedasticity is less pronounced in modern, highly precise instrumentation; and (*iii*) running a few sample replicates is common practice for the large majority of analyses, which contributes to minimizing individual standard deviation biases caused by heteroscedasticity.

Table 2 shows data on Cd and Cu determination by ICP OES that may be used as an example to evaluate how typical atomic spectrometry calibration data behave regarding normality and homoscedasticity.

The Shapiro-Wilk test is one of the most powerful formal tests to check for normality.[21,22] When applied to the residuals (e_i) of both analytes in Table 2, p values of 0.1891 and 0.1148 are found for Cd and Cu, respectively. In this case, $e_i = y_i - \hat{y}_i$, with y_i and $\hat{y}_i$ representing experimental instrument response and expected instrument response according to the estimated OLS regression coefficients, respectively. Because $p > 0.05$ for both elements, the null hypothesis of the Shapiro-Wilk test that the data comes from a normally distributed population is not rejected for either dataset. Similar results (not shown) were found for Al determination by microwave-induced plasma optical emission spectrometry (MIP OES, $p = 0.0503$), and Pt determination by ICP-MS ($p = 0.4989$). Therefore, based on different analytes and analytical methods, and as expected according to the central limit theorem,[6,18] errors in atomic spectrometry can be generally considered normally distributed.

To check for homoscedasticity, the Breusch-Pagan test may be one of the most adequate for atomic spectrometry applications.[23,24] When applied to the data in Table 2, its null hypothesis of homoscedasticity is rejected for errors (e_i) in Cu determinations ($p = 0.0396$). The Breusch-Pagan test was also applied to Al and Pt calibration data recorded by MIP OES and ICP-MS, respectively (not shown). The Al data was found homoscedastic ($p = 0.4313$), while the Pt data was heteroscedastic ($p = 0.0120$). These examples show, as discussed earlier, that atomic spectrometry data often fails to follow the third condition required to the adequate application of OLS. Table 3 shows the effects of heteroscedasticity on calibration parameters for Cu. In this case, WLS regression was applied to the data using different weighting factors (w), and the Breusch-

Pagan test was re-applied to the corrected data to check for homoscedasticity. Using $w = 1/y^{0.5}$ or $w = 1/S_y^{0.5}$ corrected the instances of heteroscedasticity, but as expected based on the work by Bohrnstedt and Carter,[20] no significant effects were observed for R^2 and accuracy when comparing OLS and WLS. Also expected,[6,25] the WLS model significantly contributed to reducing the root-mean-square error (RMSE), which is a measure of model efficiency. Similar results are shown in Table 4 for Cd, which shows that WLS can even turn data from homoscedastic into heteroscedastic when the proper weighing factor is not chosen. Table 4 also corroborates results from Table 3, as R^2 and accuracy show no significant difference between OLS and WLS, while RMSE significantly improves with WLS.

From these examples and previously published studies,[20] one may conclude that although often present in atomic spectrometry, heteroscedasticity should rarely affect accuracy. Therefore, OLS is perfectly adequate for applications involving modern quantitative spectrochemical analysis instrumentation.

Advantages and limitations of the traditional calibration methods used in atomic spectrometry

External standard calibration (EC) and matrix matching calibration (MMC)

Most quantitative instrumental methods are based on a comparison between signals from the sample and from a series of solutions of known analyte concentration (also known as calibration standards). Mathematically, calibration involves the selection of a proper model, the estimation of the functional parameters and their errors, and the validation of the model. The combination of EC and a linear function based on OLS regression is the most common approach

in modern quantitative instrumental analysis. The calibration plot is built with instrument response on the *y*-axis and analyte concentration on the *x*-axis. The slope of the calibration curve (*m*) represents the method's sensitivity. The linear function representing the relationship between instrument response and analyte concentration is then given by $y = b + mx$, where *b* is the *y*-intercept, which is associated to the blank signal. Ideally, linearity holds through several orders of analyte concentration. However, deviation from linearity is common at high analyte concentrations due to phenomena such as atomic auto-absorption. Thus, determinations at such high concentration ranges are usually not recommended for atomic spectrometry applications.

EC is the most commonly used method in routine laboratories due to its simplicity. It is so called because calibration standards (or reference solutions) are prepared and analyzed separately from the samples. Although single- and double-point procedures may be used, the more calibration points the lower the error associated with the estimated analyte concentration in the sample.[5] Despite its simplicity and effective applicability to most analyses, EC is greatly affected by the stability of the atomization process and the detection system. Due to variations in the sample environment during the analysis, additional signal correction (*e.g.* internal standardization) may be required to ensure accuracy. In addition, common instrument drift over long runs requires periodical recalibration when employing this method.

An important limitation of EC is that it assumes concomitants in the sample have negligible to no effect on the analytical signal, which is rarely the case in routine applications. Matrix is everything in the sample but the analyte. The concomitant species in the matrix may enhance or suppress the analytical signal, and because they are not present in the calibration standards, the application of EC may lead to biased results. A general example of a calibration procedure involving analytical signal suppression is presented in Fig. 1. In such cases, especially when

analyzing complex-matrix samples, EC is usually replaced by the SA method to ensure precise and accurate results. Another alternative for compensating for matrix effects, matrix matching calibration (MMC) exploits the addition of interference-causing concomitants (*e.g.* mineral acids, solvents and salts) into the calibration standard solutions to mimic the sample. Although highly efficient when the sample is closely matched, MMC is difficult to employ, as an accurate knowledge of the matrix composition is required.

Internal standardization (IS)

In atomic spectrometry measurements, fluctuations in gas flows, sample introduction aspiration rates, radiation source intensity and other instrumental parameters are generally common and may compromise precision and accuracy. One of the most common approaches to minimize the negative effects of such fluctuations on the quality of an analytical determination is the IS method. The first reference to the use of IS in atomic spectrometry was in 1877 by Gouy, who used an IS species to verify the constancy of excitation in flame emission spectroscopy.[26] Thereafter, Gerlach and Schweitezer exploited IS in 1929 to correct for random errors and enhance analytical performance in arc and spark emission spectrometry.[27] An IS species must present similar behavior to the analyte when submitted to varying conditions. More commonly, a known and constant concentration of an IS species is added to all samples, calibration standards and blank, and the analyte-to-IS signal ratio is used as dependent variable while building the calibration curve plot. In some instances, an IS species may also be added to the sample before sample preparation to account for potential losses over the course of the analytical procedure.[28]

Consider, for example, y as the instrument response, m as sensitivity, x as analyte concentration, and a as a variable depending on fluctuations in instrumental conditions (*e.g.* flame

or plasma atomizer temperature, variation in sample viscosity due to temperature or solvent variation, signal drift, etc). For an atomic spectrometry method, the following relationships can be written for the analytical (eqn (1)) and IS (eqn (2)) signals:[29]

$$y_A = m_A a_A x_A \quad (1)$$

$$y_{IS} = m_{IS} a_{IS} x_{IS} \quad (2)$$

For a given sample aliquot being analyzed and an ideal IS species, a_A and a_{IS} are equal. Assuming a constant concentration for IS, eqn (1) and eqn (2) may then be combined into eqn (3):

$$\frac{y_A}{y_{IS}} = \frac{m_A x_A}{m_{IS} x_{IS}} = R\frac{x_A}{x_{IS}} = R' x_A \quad (3)$$

where R is a response factor based on the sensitivities of the analyte and the IS, and R' incorporates the constant concentration of the IS species into R. Thus, if the IS species behaves exactly as (or closely matches) the analyte, signal fluctuations due to instrumental and environmental changes will be cancelled out, allowing for accurate and precise determinations when using the y_A/y_{IS} signal ratio and x_A to build the calibration curve.

Although efficient at minimizing signal fluctuations and contributing to more precise and accurate measurements, the use of IS to correct for matrix effects is still a topic of debate in the literature. Some authors argue that matrix matching or SA is required in combination with IS for effective signal bias correction when analyzing complex-matrix samples.[30,31] Such combination is mostly required when the IS species only partially matches the analyte's physicochemical and spectral properties. On the other hand, some studies have demonstrated significant minimization of matrix effects when using a close-to-ideal IS species. As an example in applications involving optical emission spectrometry, variations in atomization efficiency and the resulting signal enhancement or suppression due to the presence of high concentrations of carbon or easily-

ionizable elements may be resolved by internal standardization if analyte and IS species form a *homologous pair line, i.e.* if they present similar atomization, ionization and excitation energies.[32] In ICP-MS, an IS species with comparable atomic mass and ionization potential as those of the analyte may be used to compensate for matrix-based signal suppression. For example, $^{103}Rh^{+}$ (7.45 eV) is typically used as IS species in $^{107}Ag^{+}$ (7.58 eV) determinations.[33]

As expected, IS is limited by the availability of species with physicochemical and spectral properties similar to those of the analyte. In addition, the IS species must not interfere with the analyte detection, and must not be spectrally interfered by and neither react with the sample constituents. The IS method can only be used with simultaneous or fast-sequential multielement detection systems, as both analytical and IS signals must be monitored at the same time to minimize temporal fluctuations.

An ideal IS species must also be homogeneously distributed in the sample. In case of direct analysis of solids, a sample's naturally-occurring element may be used as IS species. For plant analysis by laser ablation ICP-MS (LA-ICP-MS), for example, $^{13}C^{+}$ usually is the most effective IS species compared to $^{12}C^{+}$, $^{28}Si^{+}$ and $^{31}P^{+}$ when acquiring elemental distribution images.[34] Although carbon's ionization potential is significantly higher than commonly investigated elements, its ubiquitous presence in the sample helps compensate for variations in mass sampling and sample material transportation during LA-ICP-MS determinations.

Standard additions (SA)

Matrix effects, also known as proportional bias or rotational interference, can severely affect the analytical signal in atomic spectrometry determinations. They are usually proportional

to the concentration ratio between analyte and matrix concomitants (*i.e.* the lower the ratio the more intense the matrix effect), and result in a change of the calibration curve sensitivity due to signal enhancement or suppression (Fig. 1). The SA method is a practical and well-established calibration strategy, which indiscriminately corrects for matrix effects. It was firstly used in 1937 by Hohn to determine trace elements (Cu, Pb, Zn and Fe) in an essentially pure Al sample.[26] The term "extrapolation method" was then suggested by Harvey in 1950, when SA was applied in atomic emission spectrometry.[26,35] After its application to determine Nb and Ta in ores by X-ray fluorescence spectrometry in 1954,[36] the method became popular and has since been broadly employed with most modern instrumental techniques.

In SA, the sample itself is used to prepare the calibration standards, which contributes to minimizing rotational interferences. Known and increasing amounts of a stock solution are added to distinct constant-volume aliquots of sample. The first calibration point contains the sample alone, with at least 4 or 5 additional points containing equally-spaced volumes of the added stock solution. Blank is then added to each solution to a final constant volume so that the amount of matrix is the same for all calibration standards. The instrument response (y) recorded for each of the calibration solutions can be represented as shown in eqn (4).[37]

$$y = \frac{kV_xC_x}{V_t} + \frac{kV_sC_s}{V_t} \qquad (4)$$

where k is a proportionality constant; V_x, V_s and V_t are the volumes of sample, stock solution, and the final volume of each calibration solution; and C_x and C_s are the concentrations of analyte in the sample and in the stock solution. The calibration plot is then built with instrument response on the y-axis and stock solution volumes (or analyte concentrations) added to the sample on the x-axis. Thus, the slope of the calibration curve is $m = \frac{kC_s}{V_t}$, and the intercept is $b = \frac{kV_xC_x}{V_t}$. Because C_s

and V_x are known, the concentration of analyte originally in the sample can be estimated by combining m and b and isolating C_x, as shown in eqn (5). The estimated analyte concentration in the sample can also be graphically determined, by extrapolation, as the absolute (non-negative) value for the x-axis intercept (*i.e.* when $V_S = 0$).

$$\frac{b}{m} = \frac{kV_xC_x/V_t}{kC_s/V_t} = \frac{V_xC_x}{C_s}$$

$$C_x = \frac{bC_s}{mV_x} \qquad (5)$$

SA is efficient when analyzing complex samples, especially when matrix concomitants are unknown and MMC is not feasible. For example, the determination of Si in bovine liver by graphite furnace atomic absorption spectrometry (GF AAS) after sample dissolution in tetramethylammonium hydroxide was only possible by employing SA.[38] Based on eqn (4) and eqn (5)[37], Kelly *et. al.* have also demonstrated the efficiency of the SA method in solid sample analysis.[39] Zhu and Chiba exploited gravimetric single-point SA associated with IS for ICP-MS determinations.[40] Accurate results were achieved by using an added concentration twice the value present in the sample. Although it is not possible to calculate the standard deviation of the estimated analyte concentration employing analysis of residuals, neither to check the linearity of the relationship between analyte signal and concentration, the main advantage of single-point SA is its higher analytical throughput.

It is important to note that SA assumes a linear relationship between instrumental response and analyte concentration in a given matrix. It also assumes no translational effect (*i.e.* the calibration curve line goes through the plot origin), and no variation in sensitivity as analyte is added to the sample within the analytical range. Traditionally, the analyte concentration in the sample is obtained by graphical extrapolation, which is less accurate than using interpolation. To

improve precision (*i.e.* minimize S_x), a large amount of replicates (n) and multiple instrument response values (y) are recommended (eqn (6)).[5,29]

$$s_x = \frac{s_{y/x}}{b}\sqrt{\frac{1}{n} + \frac{\bar{y}^2}{b^2 + \sum(x_i - \bar{x})^2}} \quad (6)$$

where S_x, b, x_i, $\bar{x}$ and $\bar{y}$ represent the standard deviation of the analyte concentration in the sample, the calibration curve y-intercept, an individual analyte concentration value, and the average of analyte concentration and instrument response values for all calibration standards, respectively. $S_{y/x}$ is given by $S_{y/x} = \sqrt{\sum_i (y_i - \hat{y})^2/n - 2}$, where y_i and $\hat{y}$ are an individual instrument response and the respective expected value based on the calibration curve coefficients.

More recently, the interpolation approach was systematically evaluated to assess its effect on precision and accuracy of SA determinations.[41] By interpolating the signal of the unspiked sample twice using the coefficients obtained by OLS regression, the analyte concentration in the sample was estimated using the central part of the calibration function, which minimizes both the risk of bias and the variance associated with interpolation.

The main limitation of the SA method is associated with sample throughput. In contrast to conventional EC experiments, each sample requires its own calibration curve in SA. Consequently, it is less straightforward and uses larger quantities of sample than EC. The SA method is also incapable of correcting for translational effects. When the analyte signal is affected by some component of the matrix by a fixed rate at all analyte concentrations (translational interference or background interference), the calibration curve slope is not affected, but the whole calibration line shifts in the y-direction. In such cases, the zero-intercept assumption is invalid, and an independent correction strategy must be applied to prevent biased results.

Some recently proposed strategies to improve calibration efficiency in atomic spectrometry

Interference standard method (IFS)

As previously discussed, translational interferences are not corrected by SA, IS or matrix matching approaches. In quadrupole-based ICP-MS (ICP-QMS), spectral interference from argon-, nitrogen- and oxygen-containing species, which are native to the plasma, can severely affect accuracy. Without the use of collision/reaction cells or interfaces, mathematical equations for signal correction, and/or tuning of instrumental operational conditions, ICP-QMS applications can be limited. Such interferences are especially critical because the interfering signal (I_I), which is not resolved in a typical ICP-QMS system, is usually much more intense than the analytical signal (I_A). Considering a typical Ar ICP, signal intensities for $^{38}ArH^+$ and $^{14}N_2^+$, for example, are significantly higher than those from the respective analytes $^{39}K^+$ and $^{28}P^+$. Thus, the slightest variation in I_I (V_I) between the time the calibration standards and the sample are measured causes poor recovery ($R(\%)$), as represented in eqn (7).[42]

$$R(\%) = \left(\frac{I_I}{I_A} V_I + 1\right) \cdot 100 \qquad (7)$$

The interference standard method (IFS) was proposed in 2011 to overcome such limitations and improve accuracy in ICP-QMS analyses.[42] It is based on the hypothesis that ions naturally present in the plasma such as $^{36}Ar^+$, $^{36}ArH^+$ and $^{38}Ar^+$ (IFS species) experience similar signal fluctuations as the interfering species. Therefore, the contribution from I_I to variations in the overall analytical signal (*i.e.* unresolved $I_t = I_A + I_I$ signal) can be minimized simply by dividing I_t by the IFS species signal (I_{IFS}). In practice, the mathematical treatment associated with IFS is similar to a traditional internal standardization. The analyte-to-IFS signal ratio (I_t/I_{IFS}) recorded

from the blank, calibration standards and samples are used as dependent variable on the *y*-axis, with analyte concentration as the independent variable plot on the *x*-axis. The main difference is that the IFS species ideally behaves similarly to the interfering species rather than the analyte. Thus, the IFS method minimizes spectral interferences, as it reduces the impact of the unresolved I_I on the overall I_t signal. It has been successfully employed to determine some difficult analytes such as As, K, P and Si in several sample matrices. For As determination in a 1% v/v HCl matrix by ICP-QMS, for example, a 93.5% recovery was achieved using $^{38}Ar^+$ as IFS species, which is significantly more accurate than the 147% recovery obtained with simple EC.[42]

The efficiency of the IFS method depends on the I_I/I_A ratio and on how similar V_I and V_{IFS} are, which represent the variations in signals of interfering and IFS species between the time calibration standards and samples are recorded. As shown in eqn (8), the smaller the difference between V_I and V_{IFS} (*i.e.* the more interfering and IFS species behave similarly) the more accurate the result, as the impact of any large I_I/I_A ratio on analyte recovery (*R(%)*) is neutralized. On the other hand, if V_I and V_{IFS} are not very similar, the IFS method will still be efficient if I_I/I_A is relatively small.

$$R\,(\%) = \left(\frac{1}{(1 + V_{IFS})} + \frac{I_I}{I_A} \cdot \frac{(V_I - V_{IFS})}{(1 + V_{IFS})}\right) \cdot 100 \qquad (8)$$

The core principle of the IFS method has been experimentally confirmed by high-resolution sector field double-focused ICP-MS (HR-SF-ICP-MS). It has been demonstrated that signal profiles of IFS species and interfering ions such as $^{14}N_2^+$ and $^{12}C^{16}O^+$ are similar (Fig. 2), which may be related to similar physicochemical characteristics and similar behavior when small variations in temperature, number of ions extracted, local electron density and other chemical processes take place during the analysis.[43] In the same study, $^{16}O_2^+$, $^{38}ArH^+$ and $^{40}Ar^{35}Cl^+$

interfering effects on ^{32}S, ^{39}K and ^{75}As determinations were also investigated. In addition, signal intensities from $^{38}ArH^+$ (interfering species) and $^{39}K^+$ (analyte) recorded with HR-SF-ICP-MS were combined to simulate a low resolution determination at *m/z* 39. In this experiment, the theoretical recovery calculated with eqn (8) and HR-SF-ICP-MS data including $^{36}ArH^+$ as IFS species was 106.9%. Experimentally, the $^{36}ArH^+$ ion presented the most similar behavior to the $^{38}ArH^+$ interfering species, resulting in a 102.8% analyte recovery (compared to a 61.3% recovery using EC).

Standard dilution analysis (SDA)

Among the traditional calibration methods, SA is the most effective in applications involving challenging samples. As discussed earlier, the main drawback of SA is the need for preparing a series of solutions for each individual sample. In 2015, Jones *et al.* introduced an alternative calibration method, known as standard dilution analysis (SDA), to overcome the limitations of SA and facilitate analyses of complex-matrix samples.[44] SDA combines IS and SA and requires only two calibration solutions per sample. It is based on the gradient dilution of a standard in a single container, keeping the amount of sample constant during the whole calibration process. In practice, solution 1 (S_1, with 50% sample + 50% standard solution containing the analytes and an IS element) is initially introduced into the instrument. The analytical and IS signals increase over time until a stable plateau is reached (Fig. 3). Then, solution 2 (S_2, with 50% sample and 50% blank) is slowly added into the tube containing S_1. The analytical and IS signals gradually drop, creating a negative slope as dilution takes place (SDA region of Fig. 3). Because the amount of sample remains constant while the standards are diluted (both calibration solutions have 50% sample), matrix effects are neutralized.

The SDA calibration plot is built with the analyte-to-IS signal ratio (S_A/S_{IS}) on the *y*-axis and the reciprocal of the IS concentration ($1/C_{IS}$) on the *x*-axis (Fig. 3). The values for C_{IS} at each point during the standard dilution are calculated from the maximum IS signal and from the known concentration added to S_1. The analyte concentration in the sample ($C_{A,Sam}$) is calculated from the slope and intercept of the calibration plot, and from the concentrations of the analyte ($C_{A,Std}$) and the IS (C_{IS}) in the standard originally added to S_1. Eqn (9) shows some of the general steps associated with the mathematical deductions used with the SDA method. More details can be found in the original paper by Jones *et al.*.[44]

$$\frac{S_A}{S_{IS}} = \frac{m_A[C_{A,Sam} + C_{A,Std}]}{m_{IS}C_{IS}} = \frac{m_A C_{A,Sam}}{m_{IS}C_{IS}} + \frac{m_A C_{A,Std}}{m_{IS}C_{IS}}$$

$$Slope = \frac{m_A C_{A,Sam}}{m_{IS}}$$

$$Intercept = \frac{m_A C_{A,Std}}{m_{IS}C_{IS}}$$

$$C_{A,Sam} = \frac{Slope}{Intercept} \cdot \frac{C_{A,Std}}{C_{IS}} \qquad (9)$$

where m_A and m_{IS} represent the sensitivities for the analyte and the IS element.

SDA was used, for example, to determine Al, Cd, Co, Cr, Cu, Fe, Ni and Pb in several samples by ICP OES, with accuracies comparable and mostly better than those obtained with the traditional EC, IS and SA. When considering all analytes and samples evaluated, the average percent errors of recovery (*i.e.* the percent error from the expected analyte concentration in the sample) were 19.3%, 20.3%, 10.7% and 4.7% for EC, IS, SA and SDA, respectively. The precision, calculated as relative standard deviation, was also superior for SDA. Average values based on all determinations were calculated as 19.8%, 9.3%, 13.3% and 5.8% for EC, IS, SA and SDA, respectively.[44]

It is important to note that different from IFS, SDA is incapable of correcting for spectral interferences. Therefore, it must be combined with another strategy for applications involving both rotational and translational effects. To determine As and Cr in concentrated acids by ICP-MS, for example, SDA was combined with a collision/reaction cell and tandem ICP-MS (ICP-MS/MS) to minimize not only matrix effects but also spectral interferences caused by polyatomic ions such as $^{40}Ar^{35}Cl^{+}$ and $^{35}Cl^{16}OH^{+}$. Under the same instrumental conditions, average percent recoveries for all samples and analytes evaluated were calculated as 86%, 80%, 75% and 101% for EC, IS, SA and SDA, respectively.[45]

Multi-signal methods

As mentioned at the beginning of our discussion on calibration, the traditional methods are based on a relationship between instrument response and analyte concentration. Some of the recently described multi-signal methods, such as multi-energy calibration (MEC), multi-isotope calibration (MICal), multispecies calibration (MSC) and multi-flow calibration (MFC), take advantage of dimensions associated with the analytical signal other than simply concentration, which are rarely explored for calibration[46-49] To better understand the concepts involved in these new strategies, one needs to review the parameters associated with the analytical signal generated in a modern quantitative instrumental technique. Consider, for example, the main factors contributing to analytical signal intensity in atomic emission spectrometry, which is represented in eqn (10) by the measured output potential, E_{out}, for a given emission line:[49]

$$E_{out} = \left(\frac{CF\epsilon_a}{Qe_f}\right)\frac{g_j}{g_0}e^{-E_{j0}/k_BT} \cdot VE_{j0}A_{j0}Y_mT_{op}R(\lambda)G \qquad (10)$$

where C, F, ϵ_a, Q, e_f, g_j, g_0, E_{j0}, k_B, T, V, A_{j0}, Y_m, T_{op}, $R(\lambda)$ and G represent analyte concentration, solution flow rate, atomization efficiency, nebulization gas flow rate, gas expansion factor, statistical weights of the excited state and the ground state, transition energy, Boltzmann constant, plasma temperature, volume observed by the monochromator, rate of spontaneous emission, monochromator collection efficiency, transmittance of the optics, detector responsivity, and gain of the electronics. The traditional methods simply use the relationship between E_{out} and C for calibration, incorporating all the other parameters into a proportionality constant, K, as represented in eqn (11). With the traditional methods (as well as for IFS and SDA), the analyte concentration in the sample is determined by providing a means for accurate and precise calibration interpolation. Therefore, the more calibration points used the lower the error associated with the estimated analyte concentration.[5] Thus, except for SDA, several standard solutions are prepared and run to determine the least-square regression parameters used to estimate the unknown analyte concentration in the sample.

$$E_{out} = KC \tag{11}$$

Alternatively, the multi-signal methods explore parameters such as nebulization gas flow rate, Q, and transition energy, E_{j0}, incorporating the analyte concentration into K.[46,49] In MEC, for example, a single-concentration standard is used for calibration.[46] Similar to SDA, calibration is carried out using a solution containing a mixture of sample and standard solution (1:1 v/v), and a second solution composed of half sample and half blank. No IS element is required in MEC. Each of the calibration solutions are then separately run while monitoring several wavelengths (transition energies) from the same analyte. The calibration plot is built with signals from the first and second solution on the x-axis and y-axis, respectively, and with each calibration point associated with a different transition energy. If we replace E_{out} in eqn (11) with $I(\lambda_i)$ to represent

analytical signal intensity at wavelength *i*, the relationships between analytical signal and analyte concentration for the first and second calibration solutions are:

$$I(\lambda_i)_{Sam\,+\,Std} = K\,(C_{Sam} + C_{Std}) \quad (12)$$

$$I(\lambda_i)_{Sam} = K\,C_{Sam} \quad (13)$$

where *Sam* and *Std* correspond to the sample and the standard added to the first calibration solution, respectively.

Because modern instrumentation is highly stable, negligible variation in operating conditions is expected at the different time points when analytical signals from each of the two calibration solutions are recorded. In addition, matrix effects are eliminated as both solutions have each 50% sample. Thus, *K* in eqn (12) and eqn (13) has the same constant value, and the relationship between analytical signal and concentration may be represented as:

$$I(\lambda_i)_{Sam} = I(\lambda_i)_{Sam+Std}\left[\frac{C_{Sam}}{C_{Sam} + C_{Std}}\right] \quad (14)$$

The slope of a linear least-square regression based on $I(\lambda_i)_{Sam}$ (from solution 2) *vs.* $I(\lambda_i)_{Sam\,+\,Std}$ (from solution 1), with instrument responses recorded at several different wavelengths (λ_1, λ_2, λ_3, …, λ_n), is then:

$$Slope = \left[\frac{C_{Sam}}{C_{Sam} + C_{Std}}\right] \quad (15)$$

Finally, because C_{Std} is known (as it was added to the first calibration solution), the unknown analyte concentration in the sample can be calculated by rearranging eqn (15):

$$C_{Sam} = \frac{Slope \cdot C_{Std}}{(1 - Slope)} \quad (16)$$

The 1:1 volume ratio used for the sample/standard and sample/blank calibration solutions is adopted to facilitate the application of the matrix-matched, multi-signal methods. One may employ a smaller percentage of sample (*e.g.* 20% sample and 80% standard solution or blank) to further minimize matrix effects; or a larger percentage of sample (*e.g.* 70% sample and 30% standard solution or blank) to improve the method's detectability. In such cases, no biased results are expected as long as the same amount of sample is used in both solutions. As shown in eqn (17), the only modification required to calculate the analyte concentration in the sample is the incorporation of the different volumes of sample (V_{Sam}) and standard (V_{Std}) into eqn (16). Note here that eqn (17) becomes eqn (16) when $V_{Sam} = V_{Std}$.

$$C_{Sam} = \frac{Slope \cdot C_{Std} \cdot V_{Std}}{(1 - Slope) \cdot V_{Sam}} \quad (17)$$

The same principle described for MEC is applicable to MICal and MSC, with both eqn (16) and eqn (17) suitable for any of these three calibration methods.[46-48] The main difference is that rather than multiple transition energies, MICal and MSC use signals from multiple isotopes or multiple ionic gas species of the same analyte. Fig. 4 shows typical calibration plots for MEC, MICal, MSC and MFC. In Fig. 4A, 8 emission lines are used to determine Ni in green tea by MEC-MIP OES. Using eqn (16) and considering C_{Std} = 1.00 mg L^{-1}, the Ni concentration in the sample is calculated as 0.47 mg L^{-1}, which corresponds to a 94% recovery from the original 0.50 mg L^{-1} spike. Similarly, MIcal and MSC were used to determine Cd and Co in certified reference materials (CRMs) from the National Institute of Standards and Technology (NIST, Gaithersburg, MD, USA). For Cd determination in Apple Leaves (NIST 1515), 4 isotopes were used with MICal and ICP-MS (Fig. 4B). Considering 0.100 g of sample was microwave-assisted digested with HNO_3 and H_2O_2 and diluted to 50.0 mL before analysis, and C_{Std} = 10.0 µg L^{-1}, the Cd concentration in this sample replicate is 0.0122 µg g^{-1}, a 93.8% recovery from the certified value of 0.013 ± 0.002

μg g^{-1}. In Fig. 4C, Co in Bovine Liver (NIST 1577b) is determined by tandem ICP-MS (ICP-MS/MS) using MSC and a 10.0 μg L^{-1} standard. Seven Co species produced under either O_2 or NH_3 atmosphere in the instrument's collision/reaction cell are used for calibration. For this replicate, 0.1778 g of sample was microwave-assisted digested with HNO_3 and H_2O_2 and diluted to 50.0 mL before analysis. From eqn (16), the Co concentration in the sample is calculated as 0.247 mg kg^{-1}, which corresponds to a 98.8% recovery from the certified value of 0.25 mg kg^{-1}.

MFC is based on a similar principle as the other multi-signal calibration methods. However, no matrix matching is adopted. In MFC, a single calibration standard is run while monitoring the analytical signal at a certain wavelength and at multiple nebulization gas flow rates (Q in eqn (10)). The samples are then run at the same conditions. The calibration plot is built with I_{Sam} and I_{Std} on the y-axis and x-axis, respectively, and each point in the curve is associated with a different Q. Considering that instrument response (*i.e.* I_{Sam} and I_{Std}) and analyte concentration are directly proportional at each Q condition, the slope of the MFC plot is C_{sam}/C_{std}. Thus, C_{sam} is determined by multiplying C_{std} by the calibration curve slope (eqn (18)).[49] A typical MFC plot is shown in Fig. 4D, with Q values ranging from 0.4 to 0.8 $Lmin^{-1}$. In this example, Fe in Tomato Leaves (NIST 1573a) is determined by MIP OES using a 2.00 mg L^{-1} standard solution. The mass of this sample replicate, which was submitted to microwave-assisted acid digestion and final dilution to 20.0 mL, is 0.2081 g. From eqn (18), the Fe concentration in the sample is calculated as 385 mg kg^{-1}, a 105% recovery from the 368 ± 7 mg kg^{-1} certified value.

$$C_{sam} = MFC\ Slope \cdot C_{std} \quad (18)$$

Although MFC involves no matrix-matching strategy, it may also correct for some less severe matrix effects. In MFC, samples and standards are exposed to different plasma conditions, which may result in a normalizing effect capable of improving accuracies.[49]

Main advantages and limitations of IFS, SDA and the multi-signal methods

Some of the recently proposed calibration strategies discussed here are based not only on analyte concentration but also on other parameters associated with the instrument response (Fig. 5). Successful applications of these methods, combined with several atomic spectrometry techniques, can be found in the literature. A list of studies including the analysis of complex-matrix samples such as fuels, fertilizers, alcoholic beverages and the direct analysis of solids is presented in the Table 5. In addition to providing more accurate results when compared with EC and IS, some of the most notorious advantages of SDA and multi-signal methods such as MEC, MICal and MSC over SA is their greener nature and higher sample throughputs. With accuracies comparable to SA, these methods require the preparation and analysis of fewer calibration solutions per sample, which is quicker and produces less waste. This advantage is even more evident for the direct analysis of solids, as demonstrated by studies involving laser-induced breakdown spectroscopy (LIBS). Approximately 15 samples per hour can be analyzed, with no sample decomposition required, when combining MEC and LIBS.[60,63]

SDA combines the advantages of IS and SA. Thus, matrix effects and signal fluctuations caused by variations in instrumental conditions are significantly minimized. The method can be applied to a variety of analytical instrumental techniques which accept liquid samples and are capable of simultaneous determinations. Fast sequential multielement detection is also suitable for SDA application, although limited to a smaller number of analytes per run. In such cases, the speed of solution mixing during the standard dilution process is the limiting factor to the number of

analytical signals recorded at a time. Enhanced precision is usually achieved with SDA, as it combines IS, multiple calibration points, and matrix-matching.[44] The possibility of automating SDA may contribute to even better precisions, as conditions of solution mixing can be made highly reproducible. A flow injection system (FIA) used with SDA and flame atomic emission spectrometry (FAES), for example, provided an average 2% RSD in Na determinations in biodiesel.[57]

On the other hand, an important limitation of the IFS method is that it can depreciate precision depending on the source of noise. Similar to IS, the addition of another variable (the IFS signal) may reduce precision since noise adds quadratically. In addition, large variations in the IFS signal (V_{IFS}) can compromise accuracy, as shown in the first term on the right-hand side of eqn (8). Despite such limitations, which are usually negligible in routine applications of modern instrumentation, the IFS method is simple and efficient at minimizing severe spectral interferences. It requires no instrumental modifications or addition of gases into the system, and is the only method among the ones discussed here that is capable of correcting for spectral interferences (translational effects).[42,43]

An interesting advantage of the multi-signal calibration methods is the possibility of graphically identifying spectral interferences on an analytical line, isotope or analytical species. The interfering effect will appear as a point falling outside the calibration line in MEC, MICal and MSC.[46-48] In a traditional method, such bias could only be detected after the analysis of a sample of known analyte concentration and/or by closely comparing the spectra from a standard solution and from the sample. On the other hand, systematic errors due to solution preparation are more easily detected with the traditional methods. Similar to the multi-signal strategies, an error in one of the calibration standards will appear as a point outside the calibration line for EC, IS and SA.

Because a single standard is prepared when employing SDA, MEC, MICal, MSC and MFC, an error in solution preparation will affect the entire analysis and will not be as easily detected as with the traditional methods.

It is important to realize that the multi-signal calibration methods are limited by the number of analytical wavelengths (MEC), isotopes (MICal), isotope-containing ions (MSC) and working nebulization gas flow rates (MFC) available. At least three analytical signals that are stable, sufficiently intense and free of spectral interferences must be used to obtain a calibration curve. This is less of an issue for MEC and MFC, but it may restrict MICal and MSC applications due spectral interferences and less abundant isotopes.

Calibration methods with both variables subject to error

As described earlier, the first condition to apply OLS regression is that 'o*nly the instrument response (y-axis) is subject to error. Errors in analyte concentration (x-axis) are negligible*'. This is known as Model I regression.[6] However, the multi-signal calibration methods employ instrument responses on each of the calibration axes.[46-49] Therefore, both axes are subject to error.

As detailed in the Supplementary Material, OLS is based on minimizing the differences between each experimental data point and its corresponding expected value. Because error is only expected on the dependent variable, the difference between experimental and expected values is represented as a line segment parallel to the *y*-axis of the calibration plot (Fig. 6). When error is expected on both axes, a Model II regression is more adequate than OLS.[6] Although the multi-signal calibration methods have both axes subject to error, all analytical signals originate from the same source (*i.e.* they are measured with the same analytical method), which makes their variances

likely the same. Thus, the orthogonal distance regression (ODR) model may provide the most accurate calibration coefficients in such applications.[6,64-67] ODR regression also seeks to minimize the differences between experimental and expected values, but it does so taking errors in both axes into consideration. This is achieved by minimizing the orthogonal distance between each experimental data point and the corresponding theoretical value siting on the calibration curve regression line (Fig. 6).

Although more accurate than OLS, the use of ODR may have little effect on MEC, MICal, MSC and MFC results. As shown in Table 6 and Fig. 7, regression lines are almost identical, and no significant difference is observed between analyte concentrations determined with either model. The fact that all analytical signals are measured in the same manner, no matter the calibration axis, may result in very similar errors, which render OLS as suitable as ODR for the multi-signal calibration methods. Similar to the discussion on the use of WLS *vs.* OLS, these results and the much simpler calculations involved with the latter approach allow for the efficient application of the multi-signal calibration methods without the need for ODR.

Conclusions and perspectives

An interesting trend observed in recent studies is the use of methods based on multiple measurements or multiple signal sources, which may be related to the simultaneous or fast-sequential capabilities of modern instrumental techniques. These strategies undoubtedly improve sample throughput and precision compared to SA, often providing better accuracies than all three traditional calibration methods. Although requiring at least three interference-free analytical signal

sources, the multi-signal methods have particular potential for the direct analysis of solid samples, especially in combination with LIBS and LA-ICP-MS.

Considering the level of development instrumentation has achieved in the last few years, spectral interferences increasingly become less critical in ICP-MS analysis. The use of collision/reaction cells is now almost a default step in trace element determinations. Nevertheless, the IFS method may still be relevant to laboratories with fewer resources, especially due to its simplicity and no cost of implementation. On the other hand, although incapable of correcting for spectral interferences, the SDA method can be easily employed not only with ICP-MS but also with several other instrumental techniques, and improvements associated with data processing and automation will contribute to expanding its applications and implementation in routine analyses.

The ideal calibration method is capable of significantly minimizing matrix effects, instrument-related signal fluctuations and spectral interferences, while requiring minimal amounts of samples and reagents, generating little waste, and presenting high sample throughput. Such universal calibration method has not yet been developed, so the analyst must carefully evaluate the sample, analyte and instrumentation available to decide what is the most appropriate strategy to employ in each case. The traditional calibration methods will continue to be broadly applied in atomic spectrometry due to their simplicity and robustness. However, newly described approaches such as the ones discussed in this review paper have the potential to slowly replace EC, IS and SA in some complex-matrix sample applications. These and other new strategies will contribute to faster, more accurate and precise atomic spectrometry analyses.

Conflicts of interest

There are no conflicts of interest to declare.

Acknowledgements

The authors would like to thank the National Science Foundation through its Major Research Instrumentation Program (NSF MRI, grant CHE-1531698), and the Department of Chemistry and Graduate School of Arts and Sciences at Wake Forest University for their support. The fellowship provided to R.S.A., grant 2018/23478-7, by the São Paulo Research Foundation (FAPESP) is also greatly appreciated.

References

1. J. F. Tyson, *Analyst*, 1984, **109**, 313–317.

2. E. Tognoni, M. Hidalgo, A. Canals, G. Cristoforetti, S. Legnaioli and V. Palleschi, *J. Anal. At. Spectrom.*, 2009, **24**, 655–662.

3. M. L. Shah, A. K. Pulhani, G. P. Gupta and B. M. Suri, *Appl. Optics*, 2012, **51**, 4612–4621.

4. I. B. Gornushkin, S. V. Shabanov, S. Merk, E. Tognoni and U. Panne, *J. Anal. At. Spectrom.*, 2010, **25**, 1643–1653.

5. J. C. Miller and J. N. Miller, *Statistics for Analytical Chemistry*, Ellis Horwood, Chichester, 1984.

6. D. L. Massart, B. G. M. Vandeginste, L. M. C. Buydens, S. De Jong, P. J. Lewi and J. Smeyers-Verbeke, *Handbook of Chemometrics and Qualimetrics: Part A*, Ch. 8, Straight Line Regression and Calibration, Elsevier, Amsterdam, 1997, pp. 171-230.

7. J. M. Andrade, M. J. Cal-Prieto, M. P. Gómez-Carracedo, A. Carlosena and D. Prada, *J. Anal. At. Spectrom.*, 2008, **23**, 15–28.

8. J. Andrade-Garda, *Basic Chemometric Techniques in Atomic Spectroscopy: 2 Edition*, RSC Printing, Cambridge, 2013.

9. N. B. Zorov, A. A.Gorbatenko, T. A. Labutin and A. M. Popov. *Spectrochim. Acta Part B*, 2010, **65**, 642–657

10. T. A. Labutin, S. M. Zaytsev, A. M. Popov, I. V. Seliverstova, S. E. Bozhenko, N. B. Zorov. *Spectrochim. Acta Part B*, 2013, **87**, 57–64.

11. A.-M. Legendre, *Nouvelles Méthodes pour la Détermination des Orbites des Comètes* [New Methods for the Determination of the Orbits of Comets] (in French), F. Didot, Paris, 1805.

12. K. Pearson, *The Life, Letters and Labors of Francis Galton*, Cambridge University Press, Cambridge, 1930.

13. W. G. Schrenk, *Analytical Atomic Spectroscopy*. In D. Hercules (Ed.), Modern Analytical Chemistry, Plenum Press, New York, 1975.

14. Spectroscopy Editors, *Spectrosc.*, 2006, **21**, 1–9. Available at http://www.spectroscopyonline.com/timeline-atomic-spectroscopy.

15. V. Thomsen, *Spectrosc.*, 2002, **17**, 117–120.

16. W. J. Youden, *Anal. Chem.*, 1947, **19**, 946–950.

17. H. Fischer, R. G. Hansen and H. W. Norton, *Anal. Chem.*, 1955, **27**, 857–859.

18. H. Mark and J. Workman, Jr., *Statistics in Spectroscopy*, 2nd. ed., Ch. 8. The Central Limit Theorem, Academic Press / Elsevier, San Diego, 2003.

19. W. D. Berry and S. Feldman (Ed.), *Multiple Regression in Practice*, Sage, Beverly Hills, 1985.

20. G. W. Bohrnstedt and T. M. Carter, *Robustness in Regression Analysis*, in H. L. Costner (Ed.), Sociological Methodology, Wiley, San Francisco, pp. 118–146.

21. S. S. Shapiro and M. B. Wilk, *Biometrika*, 1965, **52**, 591–611.

22. N. M. Razali and Y. B. Wah, *J. Stat. Mod. Anal.*, 2011, **2**, 21–33.

23. T. S. Breusch and A. R. Pagan, *Econometrica*, 1979, **47**, 1287–1294.

24. J. D. Lyon and C.-L. Tsai, *Statistician*, 1996, **45**, 337–349.

25. N. R. Draper and H. Smith, *Applied Regression Analysis*, 2nd ed., John Wiley and Sons, New York, 1981.

26. D. T. Burns, M. J. Walker, *Anal. Bioanal. Chem.*. 2019, **411**, 2749–2753.

27. W. Gerlach and E. Schweitezer, *Foundations and Methods of Chemical Analysis by Emission Spectrometry*, 1st ed., Adam Hilger, London, 1929.

28. D. C. Harris, *Quantitative Chemical Analysis*, 7th ed., W. H. Freeman and Company, New York, 2007, pp. 90.

29. C. Vandecasteele, C. B. Block, *Modern methods for trace element determination*, John Wiley & Sons, Chichester, 1993.

30. B. L. Batista, J. L. Rodrigues, L. Tormen, A. J. Curtius and F. Barbosa Jr., *J. Braz. Chem. Soc.*, 2009, **20**, 1406–1413.

31. E. D. Salin, M. Antler and G. Bort. *J. Anal. At. Spectrom.*, 2004, **19** , 1498–1500.

32. T. R. Dulsik, *Trace Elemental Analysis of Metals: Methods and Techniques*, CRC Press, Boca Raton, 2010.

33. C. Cascio, O. Geiss, F. Franchini, I. Ojea-Jimenez, F. Rossi, D. Gilliland and L. Calzolai. *J. Anal. At. Spectrom.*, 2015, **30**, 1255–1265.

34. K. Chacón-Madrid and M. A. Z. Arruda. *J. Anal. At. Spectrom.*, 2018, **33**, 1720–1728.

35. C. E. Harvey *Spectrochemical procedures*, Glendale: Applied Research Laboratories, In particular, 1950, p. 218–224.

36. W. J. Campbell, H.F. Carl. *Anal Chem.*, 1954, **26**, 800–805.

37. M. Bader, *J. Chem. Educ.*, **1980**, 57, 703–706.

38. S. Noremberg, M. Veiga, D. Bohrer, C. Viana, P. C. Nascimento, L. M. Carvalho and P. Mattiazzi. *Anal. Methods*, 2015, **7**, 500–506.

39. W. R. Kelly, B. S. MacDonald and W. F. Guthrie, *Anal. Chem.*, 2008, **80**, 6154–6158.

40. Y. Zhu and K. Chiba. *J. Anal. At. Spectrom.*, 2012, **27**, 1000–1006.

41. J. M. Andrade, J. Terán-Baamonde, R. M. Soto-Ferreiro and A. Carlosena. *Anal. Chim. Acta*, 2013, **780**, 13–19.

42. G. L. Donati, R. S. Amais and J. A. Nóbrega. *J. Anal. At. Spectrom.*, 2011, **26**, 1827–1832.

43. R. S. Amais, J. A. Nóbrega and G. L. Donati. *J. Anal. At. Spectrom.*, 2014, **29**, 1258–1264.

44. W. B. Jones, G. L. Donati, C. P. Calloway, Jr. and B. T. Jones. *Anal. Chem.*, 2015, **87**, 2321−2327.

45. A. Virgilio, D. Schiavo, L. M. Costa, J. A. Nóbrega, B. T. Jones and G. L. Donati, *Talanta*, 2016, **161**, 826–829.

46. A. Virgilio, D. A. Gonçalves, T. McSweeney, J. A. Gomes Neto, J. A. Nóbrega and G. L. Donati, *Anal. Chim. Acta*, 2017, **982**, 31-36.

47. A. Virgilio, J. A. Nóbrega and G. L. Donati, *Anal. Bioanal. Chem.*, 2018, **410**, 1157-1162.

48. C. B. Williams and G. L. Donati, *J. Anal. At. Spectrom.*, 2018, **33**, 762-767.

49. C. B. Williams, B. T. Jones and G. L. Donati, *J. Anal. At. Spectrom.*, 2019, **34**, 1191–1197.

50. R. S. Amais, G. L. Donati and J. A. Nóbrega, *Anal. Chim. Acta*, 2011, **706**, 223– 228.

51. R. S. Amais, G. L. Donati and J. A. Nóbrega, *J. Braz. Chem. Soc.*, 2012, **23**, 797–803.

52. G. L. Donati, R. S. Amais and J. A. Nóbrega, *J. Anal. At. Spectrom.*, 2012, **27**, 1274–1279

53. G. L. Donati, R. S. Amais and J. A. Nóbrega, *Spectroscopy*, 2012, **27**, 44–49.

54. C. D. B. Amaral, A. G. G. Dionísio, M. C. Santos, G. L. Donati, J. A. Nóbrega and Ana R. A. Nogueira, *J. Anal. At. Spectrom.*, 2013, **28**, 1303–1310.

55. M. P. Latorre, R. A. Vidal, E. González, R. Castillo, C. Pe ña-Farfal, L. D. Bennun and J. Y. Neira, *J. Chil. Chem. Soc.*, 2015, **60**, 3083–3087.

56. A. Virgilio, D. Schiavo, J. A. Nóbrega and G. L. Donati, *J. Anal. At. Spectrom.*, 2016, **31**, 1216–1222.

57. F. M. Fortunato, M. A. Bechlin, J. A. Gomes Neto, A. Virgilio, G. L. Donati and B. T. Jones, *Microchem. J.*, 2016, **124**, 662–667.

58. D. A. Gonçalves, T. McSweeney, M. C. Santos, B. T. Jones, G. L. Donati, *Anal. Chim. Acta*, 2016, **909**, 24–29.

59. A. G. Althoff, C. B. Williams, T. McSweeney, D. A. Gonçalves, and G. L. Donati, *Appl. Spectrosc.*, 2017, **1**, 2692–2698.

60. D. V. Babos, A. Virgilio, V. C. Costa, G. L. Donati and E. R. Pereira-Filho. *J. Anal. At. Spectrom.*, 2018, **33**, 1753-1762.

61. R. C. Machado, A. B. S. Silva, G. L. Donati and A. R. A. Nogueira. *J. Anal. At. Spectrom*., 2018, **33**, 1168–1172

62. A. L. Vieira, D. A. Gonçalves, A. Virgilio, E. C. Ferreira, B. T. Jones, G. L. Donati and J. A. Gomes Neto, *J. Anal. At. Spectrom.*, 2019, **34**, 972–978.

63. A. A. C. Carvalho, L. A. Cozer, M. S. Luz, L. C. Nunes, F. R. P. Rocha and C. S. Nomura, *J. Anal. At. Spectrom.*, 2019, *in press*, 10.1039/C9JA00149B.

64. J. D. Ingle and S. R. Crouch, *Spectrochemical Analysis*, Prentice Hall, Englewood Cliffs, 1988.

65. D. L. MacTaggart and S. O. Farwell, *J. AOAC Int.*, 1992, **75**, 608-614.

66. P. Glaister, *Math. Gazette*, 2001, **85**, 104-107.

67. E. C. Oliveira and P. F. Aguiar, *Quím. Nova*, 2013, **36**, 885-889.

Table 1. Overview of the traditional calibration methods and some recently described strategies covered in the present work.

Calibration method	Main characteristics	Type of correction	Main applications in atomic spectrometry
EC	Simplest, most common calibration method. Assumes negligible matrix effects.	-	FAAS, FAES, GF AAS, ICP-MS, ICP OES, LIBS, MIP OES
MMC	Interference-causing concomitants are added to the calibration standards used in EC to mimic the sample matrix.	Matrix effects	FAAS, FAES, GF AAS, ICP-MS, ICP OES, LIBS, MIP OES
IS	An internal standard species (IS) is added to calibration standards, blank and samples. The analyte-to-IS signal ratio is used for calibration.	Instrumental drift and matrix effects	FAAS, FAES, GF AAS, ICP-MS, ICP OES, LIBS, MIP OES
SA	Known and increasing amounts of analyte are added to a fixed volume of sample. The sample itself is used to prepare the calibration standards.	Matrix effects	FAAS, FAES, GF AAS, ICP-MS, ICP OES, LIBS, MIP OES

IFS	Plasma naturally-occurring species (IFS) behave similarly to interfering species and may be used for signal bias correction. The analyte-to-IFS signal ratio is used for calibration.	Spectral interferences	ICP-MS
SDA	Gradient dilution of standards in a single container produces many calibration points. It combines IS and SA. Sample matrix is constant and only two calibration standards are required per sample.	Instrumental drift and matrix effects	FAES, ICP-MS, ICP OES, MIP OES
MEC	A single concentration and multiple transition energies (wavelengths) of the same analyte are used for calibration. Sample matrix is constant and only two calibration standards are required per sample.	Matrix effects	FAES, HR-CS FAAS, HR-CS GF AAS, ICP OES, LIBS, MIP OES

MICal and MSC	A single concentration and multiple isotopes or multiple ionic species of the same analyte are used for calibration. Sample matrix is constant and only two calibration standards are required per sample.	Matrix effects	ICP-MS, ICP-MS/MS
MFC	A single standard and multiple nebulization gas flow rates are used for calibration. Plasma normalization is exploited.	Less severe matrix effects	MIP OES

Table 2. Calibration curve data for Cd and Cu determined by ICP OES.

[Cd] or [Cu] (mg L^{-1})	Instrument response, Cd (counts)	Instrument response, Cu (counts)
0	2.47	25.39
0	6.51	15.49
0	11.76	48.84
0.5	16644.86	37283.73
0.5	16622.8	36973.98
0.5	16581.44	37045.12
1.0	33177.22	74023.63
1.0	32999.36	73462.64
1.0	32598.75	73122.05
2.0	67069.48	151161.15
2.0	66836.45	150565.13
2.0	66395.98	149561.5
5.0	161326.24	374419.03
5.0	161442.38	375224.19
5.0	160128.17	371697.93
10.0	312268.82	730801.39
10.0	315453.93	732984.18
10.0	316029.11	736681.76

Table 3. Evaluation of heteroscedasticity effects on Cu determination by ICP OES.

Regression model	B-P (*p*-value)[a]	R^2	RMSE[b]	[Cu] (mg L^{-1})	Recovery (%)[c]
OLS	0.0396	0.9999	3058	2.17	109
WLS ($w = 1/y$)	0.0206	0.9999	5.853	2.16	108
WLS ($w = 1/y^2$)	0.0032	0.9999	0.01067	2.15	108
WLS ($w = 1/y^{0.5}$)	0.0884	0.9999	142.5	2.16	108
WLS ($w = 1/S_y$)	0.0429	0.9999	84.62	2.16	108
WLS ($w = 1/S_y^2$)	0.0049	0.9999	2.159	2.15	108
WLS ($w = 1/S_y^{0.5}$)	0.1274	0.9999	530.9	2.17	108

[a] Breusch-Pagan test. Homoscedastic if $p > 0.05$.

[b] Root mean of square error.

[c] Recovery from a 2.00 mg L^{-1} spike in a 1 % v/v HNO_3 matrix.

Table 4. Evaluation of heteroscedasticity effects on Cd determination by ICP OES.

Regression model	B-P (*p*-value)[a]	R^2	RMSE[b]	[Cd] (mg L^{-1})	Recovery (%)[c]
OLS	0.2345	0.9997	1843	2.02	101
WLS ($w = 1/y$)	0.0184	0.9996	8.076	1.98	99.0
WLS ($w = 1/y^2$)	0.0010	0.9995	0.02483	1.94	97.0
WLS ($w = 1/y^{0.5}$)	0.2064	0.9997	140.1	1.99	99.5
WLS ($w = 1/S_y$)	0.0066	0.9995	110.7	1.98	99.0
WLS ($w = 1/S_y^2$)	0.0011	0.9997	5.118	1.92	96.0
WLS ($w = 1/S_y^{0.5}$)	0.1411	0.9997	482.2	2.00	100

[a] Breusch-Pagan test. Homoscedastic if $p > 0.05$.

[b] Root mean of square error.

[c] Recovery from a 2.00 mg L^{-1} spike in a 1 % v/v HNO_3 matrix.

Table 5. Atomic spectrometry applications involving recently described calibration methods.

Calibration strategy	Analytes	Samples	Atomic spectrometry method	Comments	Reference
IFS	As, K, P and Si	Tap water, Apple Leaves (NIST 1515) and Typical Diet (NIST 1848a)	ICP-MS	$^{38}Ar^{+}$ IFS species improved accuracy, including As determination in a1% v/v HCl solution.	42
	Fe, Mn and S	Bovine Liver (NIST 1577b) and Typical Diet (NIST 1848a)	ICP-MS	IFS species corrected for Ar- and non-Ar-based spectral interferences (*e.g.* $^{16}O_2^{+}$).	50
	S	Lubricating oil and biodiesel	ICP-MS	Accurate determinations in high carbon-content samples (microemulsions).	51
	S and P	Lubricating oil, biodiesel and diesel	ICP-MS	High-sensitivity oxide ion detection ($^{32}S^{16}O^{+}$, $^{32}S^{16}O^{+}$, and $^{31}P^{16}O^{+}$). Superior performance for the $^{36}ArH^{+}$ IFS species.	52
	Si	Typical Diet (NIST 1848a)	ICP-MS	IFS species corrected for a non-argon-based spectral interference (*e.g.* $^{14}N_2^{+}$).	53
	As	*Brachiaria brizantha* cv. Marandu	ICP-MS	$^{83}Kr^{+}$ used as IFS species in speciation analysis of plant samples to determine As(III), As(V), DMA and MMA.	54
	Fe, Mn and Zn	Wine	ICP-MS	$^{83}Kr^{+}$ provided better results than $^{38}Ar^{+}$ as IFS species.	55
SDA	Al, Cd, Co, Cr, Cu, Fe, Ni and Pb	Mouthwash, wine, cola softdrink, nitric acid, and water	ICP OES	Lower LODs and RSDs obtained with SDA compared with the traditional methods. Y was used as IS element.	44
	As, Cd, Cr, Cu, Fe, Mn, Pb, Se and Zn	Beverages and foodstuffs	ICP OES	Relative standard deviations were better than 4.7% in all cases. Y was used as IS element.	56

	Na	Biodiesel, Non-Fat Milk Powder (NIST 1549), Whole Milk Powder (NIST 8435), Bovine Liver (NIST 1577b) and Mussel Tissue (NIST 2976)	FAES	SDA automation using flow-injection analysis (FIA). Li was used as IS element. Optical fiber probe coupled to FAES for simultaneous measurements.	57
	Al, Co, Cr, Cu, Mn, Ni and Zn	Coffee, green tea, energy drink, beer, whiskey and cachaça (Brazilian hard liquor)	MIP OES	Matrix effects and fluctuations at relatively low plasma temperatures were efficiently corrected. Y was used as IS element.	58
	As, Cr and Ni	Analytical grade and sub-boiling HNO_3 and HCl	ICP-MS/MS	As and Cr were determined as oxides species employing mass-shift mode. YO^+ was used as IS species.	45
	Al, Cr, Co, Cu, Fe, Mn, Ni and Zn	Children's cough syrup, eye drops, and oral antiseptic	MIP OES	SDA presented better precision than EC, IS and SA (up to 8-fold). Y was used as IS element.	59
MEC	Cr, Cu and Mn	Cola softdrink, cachaça (Brazilian hard liquor, *ca.* 40% v v^{-1} ethanol), apple juice, beer, and soy sauce	ICP OES	Samples were diluted in 1% v/v HNO_3 before analyses. Matrix effects due to ethanol and high carbon-content samples were corrected. MEC provided better accuracies than EC, IS and SA.	46
	Cr, Cu and Ni	Creek and drinking waters, green tea, cola soft drink, tap water and cough medicine	MIP OES		
	Co, Fe and Ni	Ethanol fuel, vinegar, and red wine	HR-CS FAAS		
	Ca, Cu, Fe, Mn and Zn	Mineral supplements for cattle	LIBS	Na_2CO_3 was used as blank (diluent). Relatively high analytical throughput (15 samples h^{-1}).	60

	As, Ba, Cd, Cr, and Pb	Fertilizers	MIP OES	Cd was not accurately determined at low concentration due to spectral interferences or low sensitivity of the emission lines.	61
	N, P and S	Liquid fertilizer, Whole Milk Powder (NIST 8435) and Non-Fat Milk Powder (NIST1549)	HR-CS FMAS and HR-CS GF MAS	Molecular absorption was monitored (more than 10 band heads for each analyte).	62
	Al, Fe and Ti	Brick clay and sediment	LIBS	High-Si samples prepared by borate fusion to improve sample homogeneity. B and Li used as IS elements.	63
MICal	Ba, Cd, Se, Sn, and Zn	Apple (NIST 1515), Peach (NIST 1547), Spinach (NIST 1570a) and Tomato Leaves (NIST 1573a), Wheat (NIST 1567a) and Rice Flours (NIST 1568b), and Trace Element in Water (NIST 1643e)	ICP-MS	Spectral interferences on a given isotope can be easily detected.	47
MSC	As, Co and Mn	Bovine Liver (NIST 1577b) and pork liver, Tomato Leaves (NIST 1573a), and white and brown rice	ICP-MS/MS	Both oxide and ammonia-cluster species were used to build the MSC curve for each analyte.	48
MFC	Cr, Cu, Fe and Mn	Secondary Drinking Water (HPS), River Sediment A (HPS), Tomato Leaves (NIST 1573a), oat cereal, oatmeal and sea and river water	MIP OES	Matrix effects were minimized due to plasma normalization at different nebulization gas flow rates. RSD values are generally lower than those obtained with EC.	49

Table 6. Effect of the regression model adopted on the accuracy of the multi-signal calibration methods. Concentration values are reported as mean ± 1 standard deviation (mg kg^{-1}, n = 3). Several non-significant figures are shown to facilitate the visualization of differences between OLS and ODR results.

Sample	Analyte	Calibration method	OLR	ODR	%difference
Tomato Leaves[a]	Co	MSC[b]	0.570319 ± 0.014578	0.570328 ± 0.014579	-0.0014
Bovine Liver[c]	Mn	MSC[b]	11.960 ± 0.794	11.961 ± 0.795	-0.013
Water Pollution Standard 1[d]	Cr	MEC[e]	98.089 ± 0.855	98.096 ± 0.853	-0.0066
Children cough syrup	Cu	MEC[e]	0.517245 ± 0.002616	0.517248 ± 0.002619	-0.00069
River sediment A[f]	Cu	MFC[e]	0.9582 ± 0.0157	0.9585 ± 0.0156	-0.025
Tomato Leaves[a]	Mn	MFC[e]	262.8 ± 12.5	262.0 ± 12.6	-0.089

[a] NIST 1573a. [b] Determination by ICP-MS/MS.[48] [c] NIST 1577b. [d] VHG Labs (Manchester, NH, USA). [e] Determination by MIP OES.[46,49] [f] High Purity Standards (Charleston, SC, USA).

Figure captions

Fig 1. Effect of the sample matrix on EC curves and on accuracy.

Fig. 2. Signal intensity variation for interfering ions ($^{14}N_2^+$ + $^{12}C^{16}O^+$) and $^{36}Ar^+$ (**A**), $^{36}ArH^+$ (**B**) and $^{38}Ar^+$ (**C**) IFS species recorded with HR-SF-ICP-MS while introducing Si solutions prepared in 1% v/v HNO_3. Measurements 1, 3, 5, 7, 9 and 11 correspond to blank, 20, 50, 100, 200 and 500 µg L^{-1} Si calibration standards, respectively. Measurements 2, 4, 6, 8, 10 and 12 correspond to tap water diluted in 1% v/v HNO_3 (0.1:10) containing Si concentrations of 0, 20, 50, 100, 200 and 500 µg L^{-1}, respectively. (Reproduced from ref. 43 with permission from The Royal Society of Chemistry.)

Fig. 3. Generic time-resolved SDA plots (left) depicting signal intensities for analytes 1, 2 and 3 and the internal standard (IS). The graph on the right shows the respective SDA calibration curves for each analyte.

Fig. 4. Typical multi-signal calibration plots. (**A**) Determination of a 0.50 mg L^{-1} Ni spike in green tea by MEC-MIP OES using a 1.00 mg L^{-1} standard solution.[46] Each calibration point corresponds to a different emission wavelength. (**B**) Cadmium determination in Apple Leaves (NIST 1515) by MICal-ICP-MS using a 10.0 µg L^{-1} standard solution.[47] Each calibration point corresponds to a different Cd isotope represented by its mass-to-charge ratio (*m/z*). (**C**) Cobalt determination in Bovine Liver (NIST 1577b) by MSC-ICP-MS/MS using a 10.0 µg L^{-1} standard solution.[48] Each calibration point corresponds to a different Co species. (**D**) Iron determination in Tomato Leaves (NIST 1573a) by MFC-MIP OES using a 10.0 µg L^{-1} standard solution.[49] Each calibration point corresponds to a different nebulization gas flow rate.

Fig. 5. Schematic representation of some recently described calibration methods and their principles.

Fig. 6. Generic calibration plot showing regression lines for OLS and ODR. An example of how differences between experimental and expected values are calculated in OLS and ODR is shown as segment lines connecting one of the calibration points and the respective regression lines. Both regression models seek to minimize the length of such segment lines for all data points.

Fig. 7. Comparison between OLS and ODR for Mn determination in Tomato Leaves (NIST 1573a) by MFC.[49]

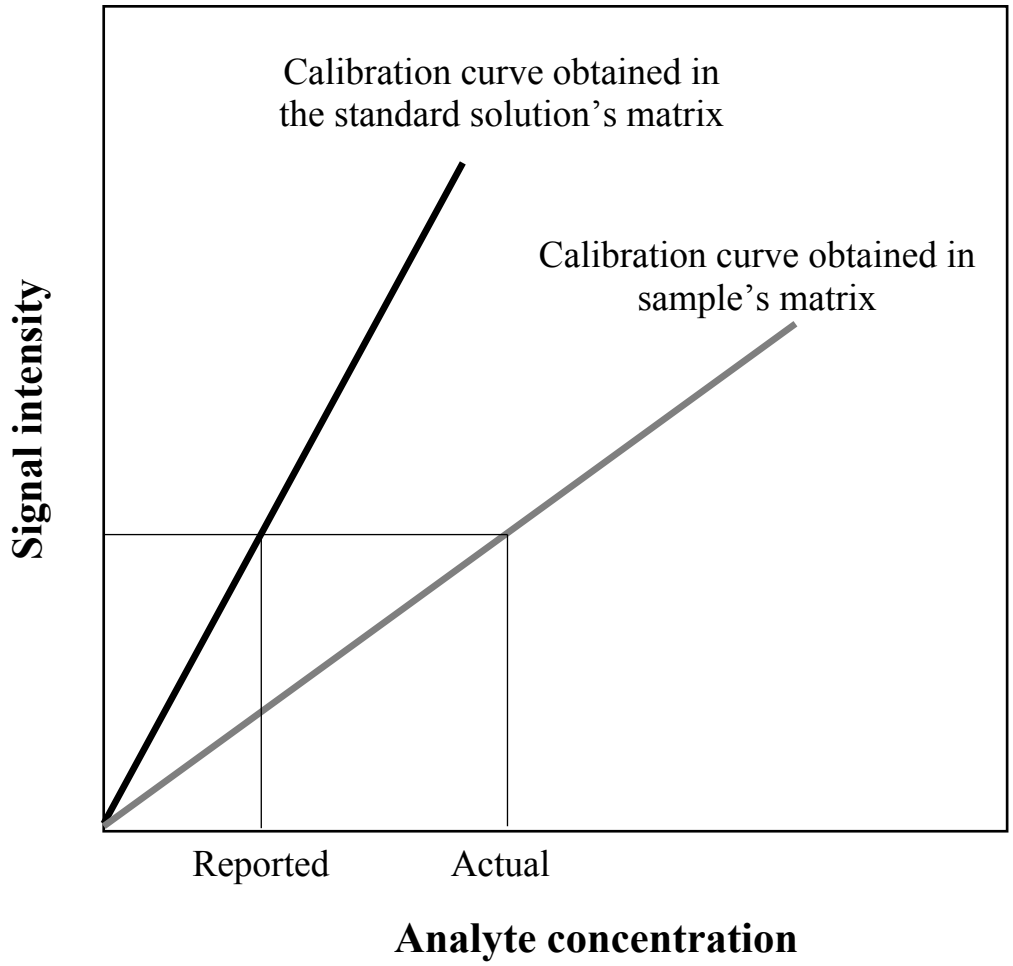
Calibration curve obtained in
the standard solution's matrix
Calibration curve obtained in
sample's matrix
Signal intensity
Reported
Actual
Analyte concentration

Fig. 1

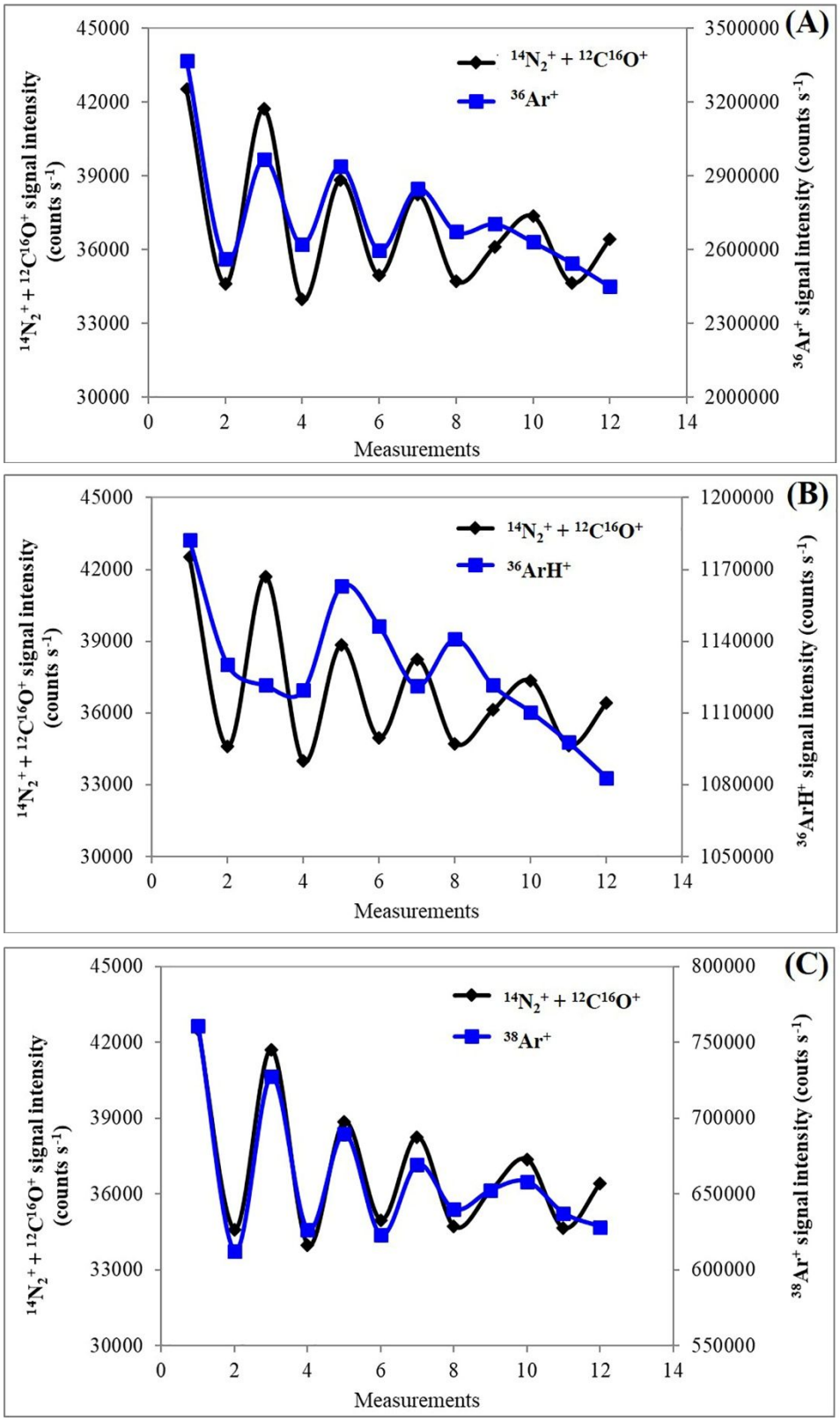
(A)
$^{14}N_2^+ + {}^{12}C^{16}O^+$
$^{36}Ar^+$
$^{14}N_2^+ + {}^{12}C^{16}O^+$ signal intensity (counts s^{-1})
$^{36}Ar^+$ signal intensity (counts s^{-1})
Measurements
(B)
$^{14}N_2^+ + {}^{12}C^{16}O^+$
$^{36}ArH^+$
$^{14}N_2^+ + {}^{12}C^{16}O^+$ signal intensity (counts s^{-1})
$^{36}ArH^+$ signal intensity (counts s^{-1})
Measurements
(C)
$^{14}N_2^+ + {}^{12}C^{16}O^+$
$^{38}Ar^+$
$^{14}N_2^+ + {}^{12}C^{16}O^+$ signal intensity (counts s^{-1})
$^{38}Ar^+$ signal intensity (couts s^{-1})
Measurements

Fig. 2

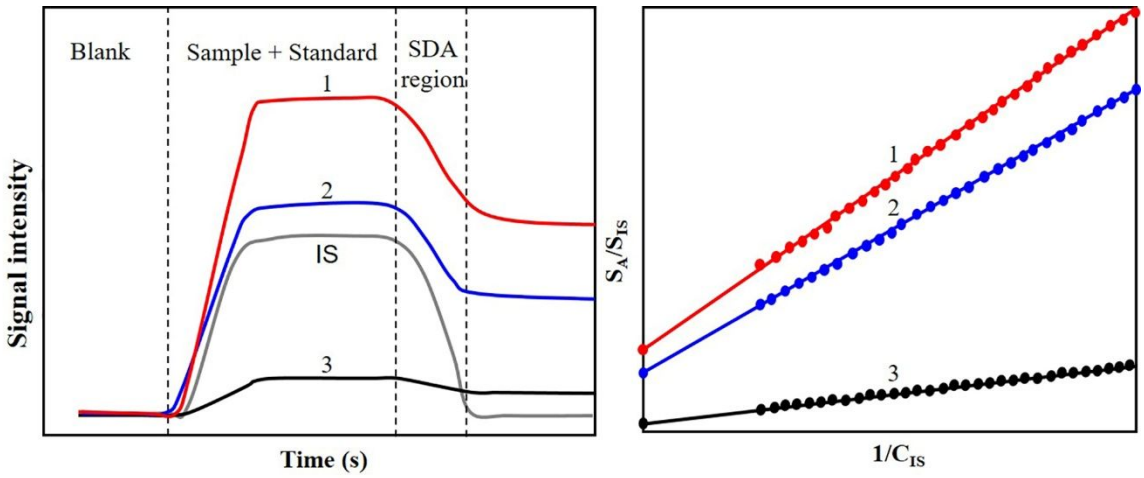
Blank
Sample + Standard
SDA region
1
2
IS
3
Signal intensity
Time (s)
S_A/S_{IS}
1
2
3
$1/C_{IS}$

Fig. 3

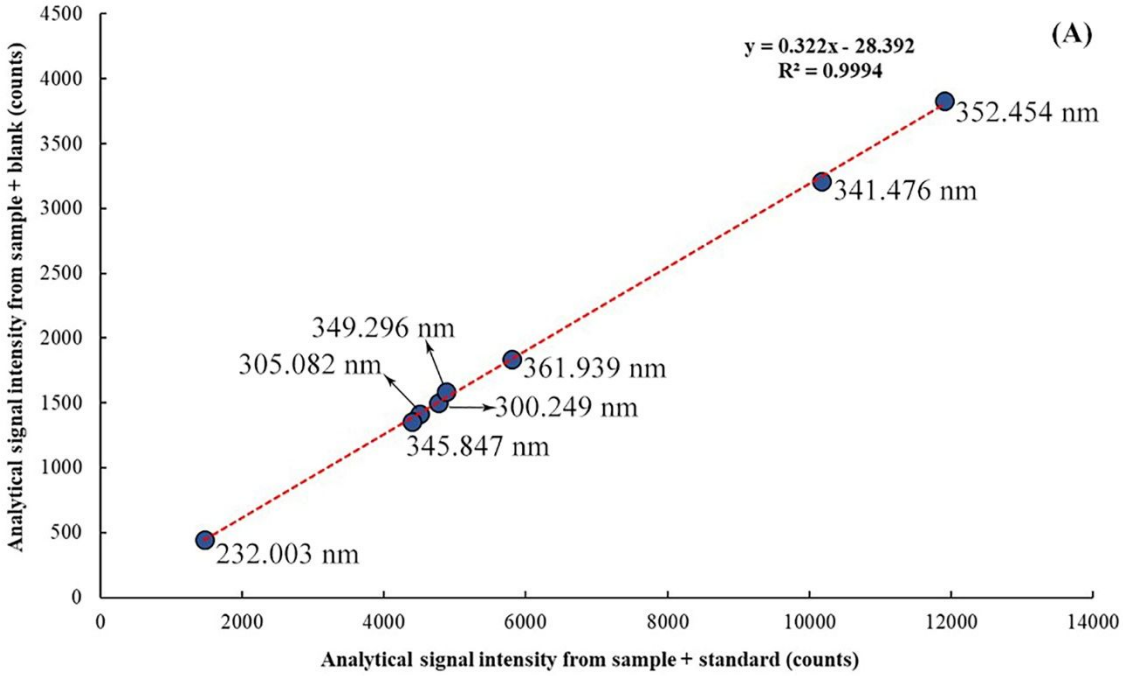
(A)
y = 0.322x - 28.392
R² = 0.9994
352.454 nm
341.476 nm
349.296 nm
305.082 nm
361.939 nm
300.249 nm
345.847 nm
232.003 nm
Analytical signal intensity from sample + blank (counts)
Analytical signal intensity from sample + standard (counts)
0
500
1000
1500
2000
2500
3000
3500
4000
4500
0
2000
4000
6000
8000
10000
12000
14000

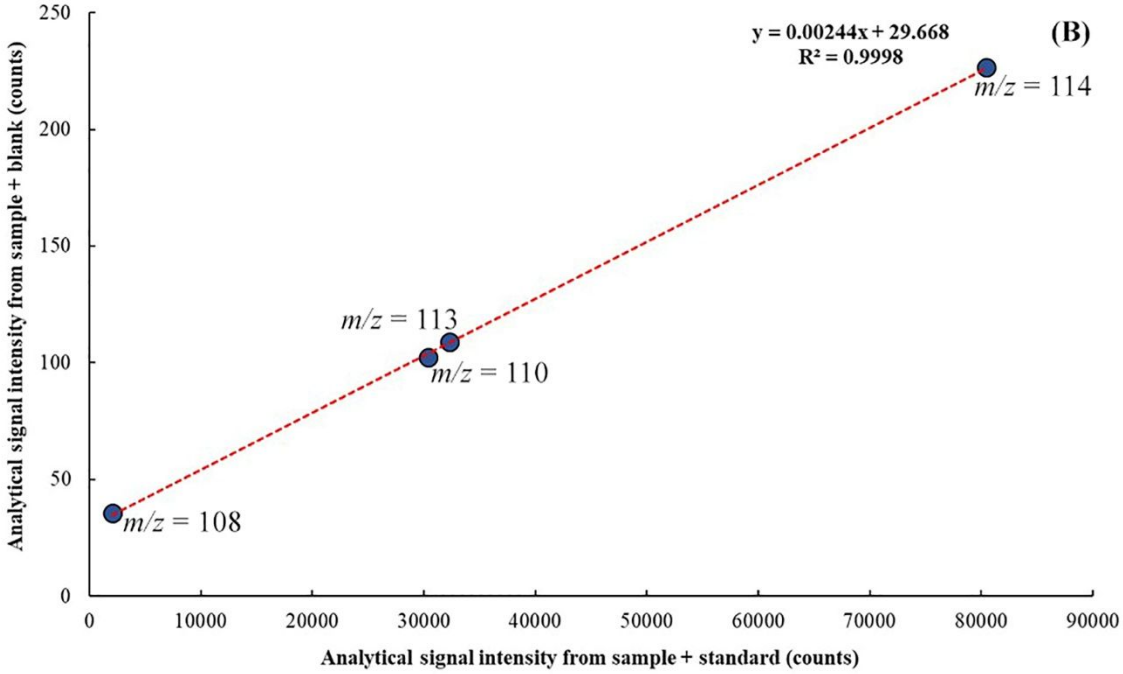
(B)
y = 0.00244x + 29.668
R² = 0.9998
m/z = 114
m/z = 113
m/z = 110
m/z = 108
Analytical signal intensity from sample + blank (counts)
Analytical signal intensity from sample + standard (counts)
0
50
100
150
200
250
0
10000
20000
30000
40000
50000
60000
70000
80000
90000

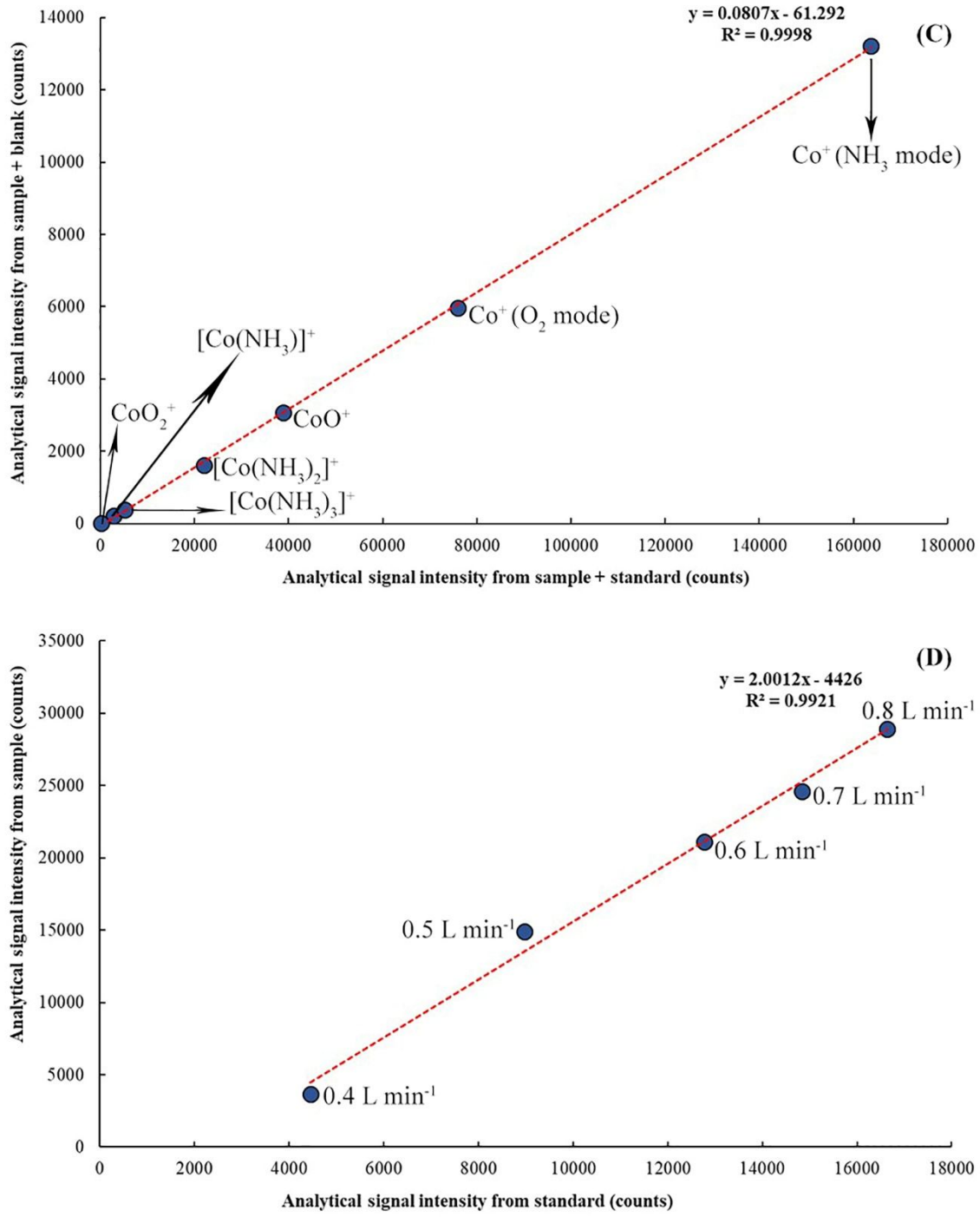
y = 0.0807x - 61.292
R² = 0.9998
(C)
Co⁺ (NH₃ mode)
Co⁺ (O₂ mode)
[Co(NH₃)]⁺
CoO₂⁺
CoO⁺
[Co(NH₃)₂]⁺
[Co(NH₃)₃]⁺
Analytical signal intensity from sample + blank (counts)
Analytical signal intensity from sample + standard (counts)
0
2000
4000
6000
8000
10000
12000
14000
0
20000
40000
60000
80000
100000
120000
140000
160000
180000
y = 2.0012x - 4426
R² = 0.9921
(D)
0.8 L min⁻¹
0.7 L min⁻¹
0.6 L min⁻¹
0.5 L min⁻¹
0.4 L min⁻¹
Analytical signal intensity from sample (counts)
Analytical signal intensity from standard (counts)
0
5000
10000
15000
20000
25000
30000
35000
0
2000
4000
6000
8000
10000
12000
14000
16000
18000

Fig. 4

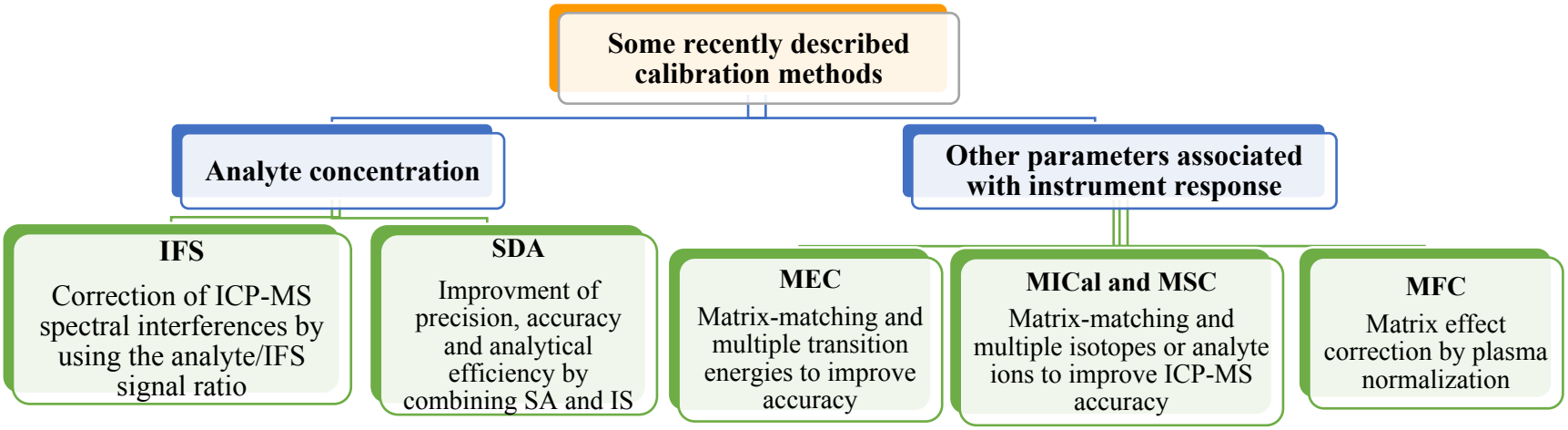
Some recently described calibration methods
Analyte concentration
Other parameters associated with instrument response
IFS
Correction of ICP-MS spectral interferences by using the analyte/IFS signal ratio
SDA
Improvment of precision, accuracy and analytical efficiency by combining SA and IS
MEC
Matrix-matching and multiple transition energies to improve accuracy
MICal and MSC
Matrix-matching and multiple isotopes or analyte ions to improve ICP-MS accuracy
MFC
Matrix effect correction by plasma normalization

Fig. 5

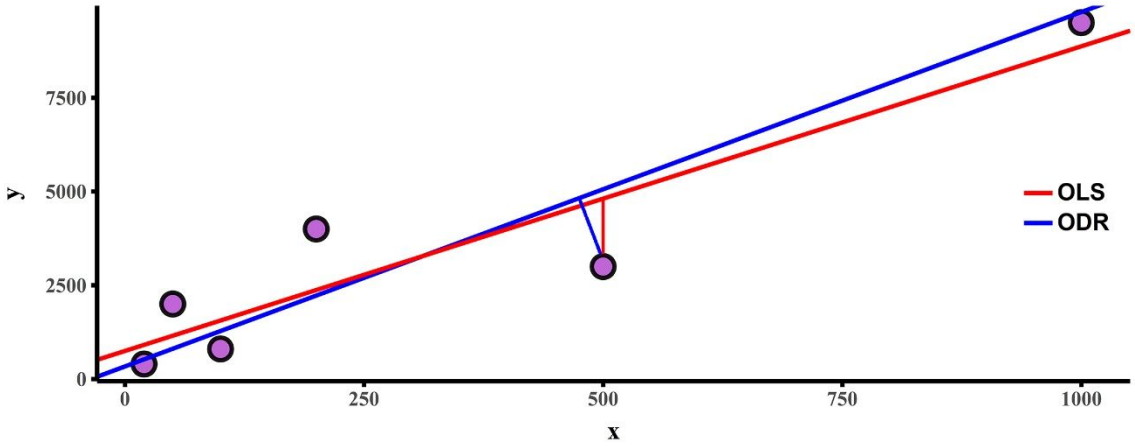

Fig. 6

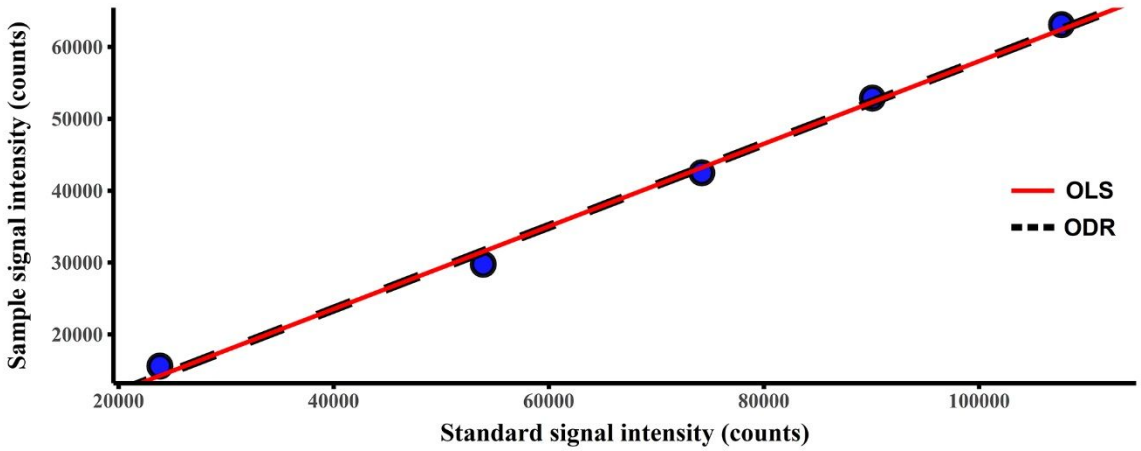
Sample signal intensity (counts)
60000
50000
40000
30000
20000
20000
40000
60000
80000
100000
Standard signal intensity (counts)
OLS
ODR

Fig. 7